Effect of Transjunctional KCl Gradients on the Spermine Inhibition of Connexin40 Gap Junctions

Xianming Lin and Richard D. Veenstra

Department of Pharmacology, The State University of New York Upstate Medical University, Syracuse, New York

ABSTRACT   Spermine inhibits rat connexin40 (Cx40) gap junctions. Glutamate residues at positions 9 and 13 and a basic amino acid (HKH) motif at positions 15–17 on the amino terminal domain are essential for this inhibitory activity. Questions remain as to whether spermine occludes the channel within the ion permeation pathway. To examine this question, *cis* or *trans* [KCl] was systematically lowered and the equilibrium dissociation constants (K_d) and kinetics of unilateral spermine block on wild-type Cx40 gap junctions were determined. Asymmetric reductions in the *trans* [KCl] produced noticeable asymmetric shifts in the $V_{1/2}$ and G_{min} values that progressively resembled G_j-V_j relationships observed in heterotypic connexin gap junction combinations. As *cis* or *trans* [KCl] was reduced by 25%, 50%, or 75% relative to the spermine-containing side, the transjunctional voltage (V_j)-dependent K_d values increased or decreased, respectively. The spermine on-rates and off-rates, calculated from the junctional current decay and recovery time constants, were similarly affected. Hill coefficients for the spermine dose-response curves were ~0.58, indicative of negative cooperativity and possible multiple spermine inhibitory sites. The equivalent "electrical distance" (δ) ranged from 0.61 at 25% *cis* [KCl] to 1.4 at 25% *trans* [KCl], with a Hill coefficient of 1.0. Symmetrical reductions in [KCl] resulted in intermediate decreases in the spermine K_ds, indicative of a minor electrostatic effect and a more significant effect of the transjunctional KCl electrodiffusion potential on the spermine association and dissociation rates. These data are consistent with a single spermine molecule being sufficient to occlude the Cx40 gap junction channel within the KCl permeation pathway.

INTRODUCTION

Gap junctions functionally integrate coupled cells via electrical and chemical diffusion of ions and second messengers by forming aqueous pores between like cells that directly mediate intercellular communication. Gap junctions can be regulated by a variety of cellular signals, including transjunctional voltage (V_j), intracellular Ca^{2+} and proton concentrations, and receptor signaling cascades (1,2). Recent reports also suggest that Mg^{2+} and intracellular polyamine levels can modulate gap junction conductance (g_j) (3–7). Polyamines are ubiquitous aliphatic amines that are positively charged under physiological conditions and are expected to interact with negatively charged molecules, such as nucleic acids, phospholipids, or proteins within the cells. They may have a dual role in cellular function by promoting cell growth or inducing apoptosis when they occur in excess (8–10). They may also specifically interact with certain ion channels, such as Ca^{2+}-permeable glutamate receptors, *N*-methyl-D-aspartate receptors, cardiac ryanodine receptors, inward rectifying potassium channels, cyclic nucleotide–gated channels, and Na^+ channels (11–17).

Spermine is the only polyamine known to significantly block connexin40 (Cx40) gap junctions in the physiological submillimolar range, and it does so in a concentration- and

V_j-dependent manner (6). Two glutamate residues at positions 9 and 13 and a basic amino acid (HKH) motif at positions 15–17 on the amino terminal (NT) domain are essential for this inhibitory activity (18,19). Two cytoplasmic glutamate residues on the BK channel subunit dramatically facilitate Mg^{2+} or spermine block by a primarily electrostatic mechanism (20). Polyamine blockade of ion channels most commonly involves electrostatic interactions with acidic or neutral polar amino acids within or near the channel pore (12,21–24), but allosteric effects on NMDA receptor channel gating are also known to occur (25). Since spermine reduces Cx40 gap junction channel activity with only minor effects on channel conductance, it is important to determine whether the spermine inhibitory site resides within the Cx40 gap junction channel ion permeation pathway or acts by an allosteric mechanism.

Asymmetrical alterations to the transjunctional salt gradient for permeable ions will result in an electrochemical diffusion potential across the Cx40 gap junction, even when two coupled cells are voltage clamped to the same membrane potential (19). If spermine occlusion of the Cx40 gap junction channel occurs within the permeation pathway, then altering the net transjunctional KCl fluxes will affect the equilibrium and kinetic properties of spermine block. In this study, we lowered *cis* or *trans* [KCl] and determined the effects of transjunctional [KCl] gradients on the spermine inhibition of Cx40 gap junctions. We demonstrate that lowering *trans* [KCl] decreased the spermine equilibrium constant (K_d), whereas a relative increase in the *trans* [KCl] increased the inhibitory K_d. The kinetics and electrical distance (δ) were

also similarly affected by the altered *cis-trans* [KCl] gradients. Symmetrically lowering [KCl] also enhanced the amount of spermine block, but the observed effects were lesser than those observed with asymmetrical lowering of the *trans* or *cis* [KCl]. The results indicate that K^+ and spermine interact at a common site or sites and that one spermine molecule is sufficient to completely occlude the Cx40 gap junction channel within the KCl permeation pathway.

MATERIALS AND METHODS

All dual whole-cell voltage-clamp experiments were performed on stable rat Cx40 transfected N2a cell cultures on the stage of an inverted phase-contrast microscope (IMT-2, Olympus, Melville, NY) using two RK-400 patch-clamp amplifiers (Molecular Kinectics, Pullman, WA), as previously described (25). The standard KCl internal pipette solution (IPS) contained (in mM) KCl 140, $MgCl_2$ 1.0, $CaCl_2$ 3.0, K_4BAPTA 5.0, and Hepes 25, pH 7.4 (titrated with 1 N KOH). The final osmolarity of all external and internal solutions was adjusted to 310 mOsm with 1 M KCl. Raffinose (Sigma Chemical, St. Louis, MO) was added to each low [KCl] IPS to maintain the osmolarity at 310 mOsm. The K^+ activities of each IPS were measured using ion-selective electrodes. MgATP was added daily to achieve a final concentration of 3.0 mM. A stock solution of 0.5 M spermine$(HCl)_4$ (Calbiochem, La Jolla, CA) was diluted daily, as required, with IPS KCl. Errors in the transjunctional voltage command signal ($V_j = V_1 - V_2$) resulting from the series resistance of each patch electrode (R_{el}) and the actual junctional conductance (g_j) calculations were calculated according to (26)

$$g_j = -\Delta I_2 / ((V_1 + \Delta V_1) - (I_1 \times R_{el1}) - V_2 + (I_1 \times R_{el1})). \quad (1)$$

Whole-cell currents were digitized at 1 or 4 kHz after low-pass filtering at 100 or 500 Hz with a four-pole Bessel filter (LPF- 202 A, Warner Institute, Hamden, CT). All currents analysis and curve-fitting procedures were performed using Clampfit software (pCLAMP version 8.2, Axon Instruments) using the sum of squared errors minimization procedure. Final graphs were prepared using Origin version 6.1 or 7.5 software (OriginLab, Northampton, MA).

The membrane potential of the spermine$(HCl)_4$ + KCl-containing cell (V_1) was stepped (ΔV_1) to negative (control), positive (block), and back to negative (recovery) V_j values relative to the common holding potential (-40 mV $= V_2$). A 500 ms s step to -40 mV occurred 20 s into each V_j pulse to assess any change in the whole-cell current baseline from which the junctional current ($I_j = -\Delta I_2$) was measured. V_j was varied in increasing 5-mV increments to ± 50 mV. The duration of each V_j step was 30 s, with a 10-s rest interval between each $-/+/-$ voltage sequence.

RESULTS

Effects of KCl on V_j gating and equilibrium binding properties of spermine inhibition

The primary purpose of this study was to determine whether transjunctional [KCl] gradients alter the V_j-dependent spermine-blocking properties of homotypic Cx40 gap junctions. In previous studies, the fraction of unblocked steady-state junctional current ($I_{j(KCl+spermine)}/I_{j(KCl)}$) was calculated by dividing the steady-state I_j obtained at positive V_j by the steady-state I_j obtained at the equivalent negative V_j for each experiment (6,18,19). This procedure for calculating the amount of spermine inhibition is valid provided that the I_j responses are otherwise similar in response to V_j steps of positive and

negative polarity, i.e., symmetrical. To account for the asymmetric V_j-dependent gating produced by the unilateral reductions in [KCl], steady-state junctional conductance-voltage curves were determined from Cx40-N2a cell pairs under all three symmetrical and unilateral low [KCl] conditions. The V_j-dependent gating of gap junctions was described by fitting the g_j obtained for each V_j polarity with a two-state Boltzmann equation:

$$g_j = (g_{max} \times (\exp(A \times (V_j - V_{1/2}))) + g_{min})/ \\ (1 + (\exp(A \times (V_j - V_{1/2})))), \quad (2)$$

where g_{min} is the residual voltage-insensitive portion of g_j achieved over the examined V_j range, g_{max} is the normalized maximum slope conductance (obtained at low V_j values, e.g., ± 5 to ± 25 mV), $V_{1/2}$ is the half-inactivation voltage for the voltage-sensitive portion of g_j, and A is the slope factor for the curve. $A = zq/kT$ where q is the equivalent charge of an electron, z is the valence of the voltage sensor, k is Boltzmann's constant, and T is the absolute temperature (°K) for the experiment. The normalized G_j was obtained by dividing g_j by the g_{max} value for each V_j polarity. The results in Fig. 1 and Table 1 describe the shift in the V_j-dependent equilibrium gating properties associated with homotypic Cx40 gap junctions under asymmetric [KCl] conditions. The resultant shifts in the V_j gating properties are reminiscent of those observed when heterotypic gap junctions are formed between two different connexins possessing different NT-domain charged amino acid residues in the same corresponding sequence positions (18,27–29).

Control spermine inhibition dose-response curves were obtained in response to spermine added unilaterally to the cell receiving the voltage-clamp pulses (cell 1 = *cis* = spermine-containing side of the junction $= I_1$), as previously described under symmetric conditions with 140 mM KCl (6). Fig. 2 *A* demonstrates the increasing time- and V_j-dependent inhibition of Cx40 double whole-cell gap junctional currents (I_j) by 2 mM spermine during increasingly positive V_j pulses from a single experiment. The symmetrical [KCl] dose-response curve data were fitted with the equation

$$I_{j(KCl+spermine)}/I_{j(KCl)} = 1/\left(1 + \left([spermine]/K_d^{eff}\right)^n\right), \quad (3)$$

where n is the Hill coefficient. Representative V_j-dependent dose-response curves obtained under symmetric 140 mM KCl conditions are illustrated in Fig. 2 *D*. The V_j-dependent K_d values decreased as [KCl] was symmetrically lowered, whereas the Hill coefficient for spermine inhibition remained essentially constant at 0.6 (Table 2 and Supplementary Material, Table S1). Applying these same procedures to the spermine inhibition-concentration curves obtained under asymmetric [KCl] conditions would yield an "apparent K_d" (K_d^{app}) based on the assumption of symmetrical I_j responses in the absence of spermine (data not shown). As illustrated in Fig. 1, the V_j-dependent gating of rat Cx40 gap junctions was not symmetrical when *cis* or *trans* [KCl] was unilaterally
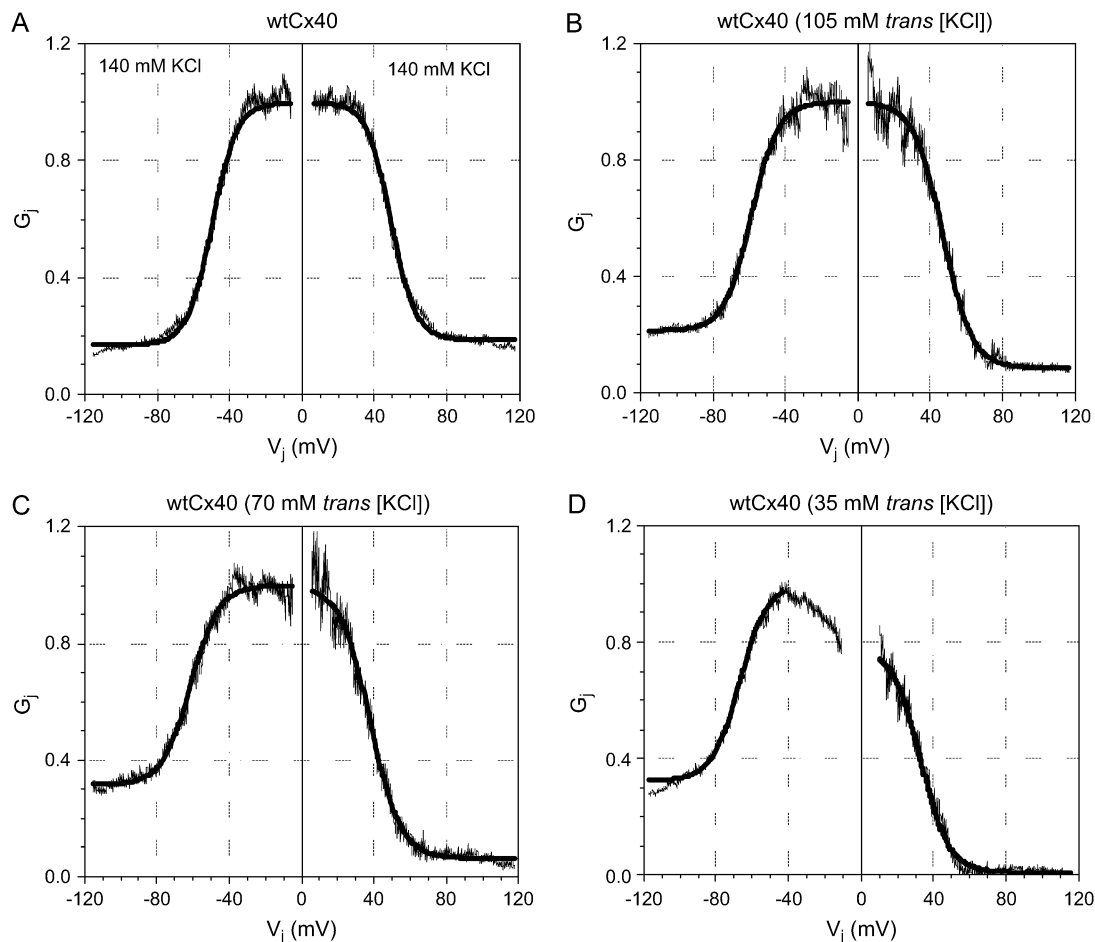
FIGURE 1 Cx40 G_j-V_j relationships under asymmetric normal to low [KCl] conditions. The steady-state G_j-V_j curves from six experiments under symmetrical control (A), asymmetric 75% *trans* [KCl] (B), asymmetric 50% *trans* [KCl] (C), and asymmetric 25% *trans* [KCl] conditions (D) are shown. The positive and negative V_j polarities of each curve were fit by Eq. 2 (*thick solid line*) and the results are presented in Table 1. Under asymmetric [KCl] conditions, the G_{min} and $V_{1/2}$ progressively increased on the low-[KCl] side while concomitantly decreasing on the high-[KCl] side.

reduced in accordance with the experimental conditions employed in this study. To account for these [KCl]-dependent changes in V_j gating when assessing the amount of spermine block in a given experiment, we fitted the steady-state g_j-V_j curves produced under asymmetric [KCl] conditions with the Boltzmann equation,

$$
\begin{aligned}
I_j &= g_j \times V_j \\
&= V_j \times (g_{j,max} \times (\exp(A \times (V_j - V_{1/2}))) + g_{j,min})/ \\
&\quad (1 + (\exp(A \times (V_j - V_{1/2})))),
\end{aligned} \tag{4}
$$

using the appropriate values from Table 1. The $g_{j,max}$ value for each experiment was determined from slope conductance

TABLE 1 V_j-dependent gating parameters for Cx40 gap junctions with low *trans* [KCl]

Parameter	Control $-V_j^*$	Control $+V_j^*$	75% *trans* [KCl] $-V_j^*$	75% *trans* [KCl] $+V_j^*$	50% *trans* [KCl] $-V_j^*$	50% *trans* [KCl] $+V_j^*$	25% *trans* [KCl] $-V_j^*$	25% *trans* [KCl] $+V_j^*$
G_{max}	$1.0^{\dagger}$	$1.0^{\dagger}$	$1.0^{\dagger}$	$1.0^{\dagger}$	$1.0^{\dagger}$	$1.0^{\dagger}$	$1.33^{\ddagger} \pm 0.005$	$1.16^{\ddagger} \pm 0.003$
G_{min}	0.17 ± 0.001	0.19 ± 0.001	0.22 ± 0.002	0.09 ± 0.002	0.32 ± 0.002	0.06 ± 0.002	0.38 ± 0.002	0.03 ± 0.002
$V_{1/2}$ (mV)	-49.7 ± 0.1	$+49.2 \pm 0.1$	-59.0 ± 0.1	$+47.0 \pm 0.1$	-61.3 ± 0.1	$+37.9 \pm 0.1$	-66.8 ± 0.1	$+30.0 \pm 0.1$
Valence (q)	3.71 ± 0.03	3.78 ± 0.03	3.41 ± 0.04	3.17 ± 0.04	3.23 ± 0.04	3.03 ± 0.04	2.74 ± 0.03	2.52 ± 0.03
Correlation coefficient (r)	0.96	0.96	0.95	0.92	0.96	0.91	0.97	0.93
N		6		6		6		6

*V_j is defined relative to the 100% (140 mM) KCl-containing cell.
$^{\dagger}G_{max}$ was fixed to a value of 1.0 at $V_j = 0$ mV for the indicated curve fit.
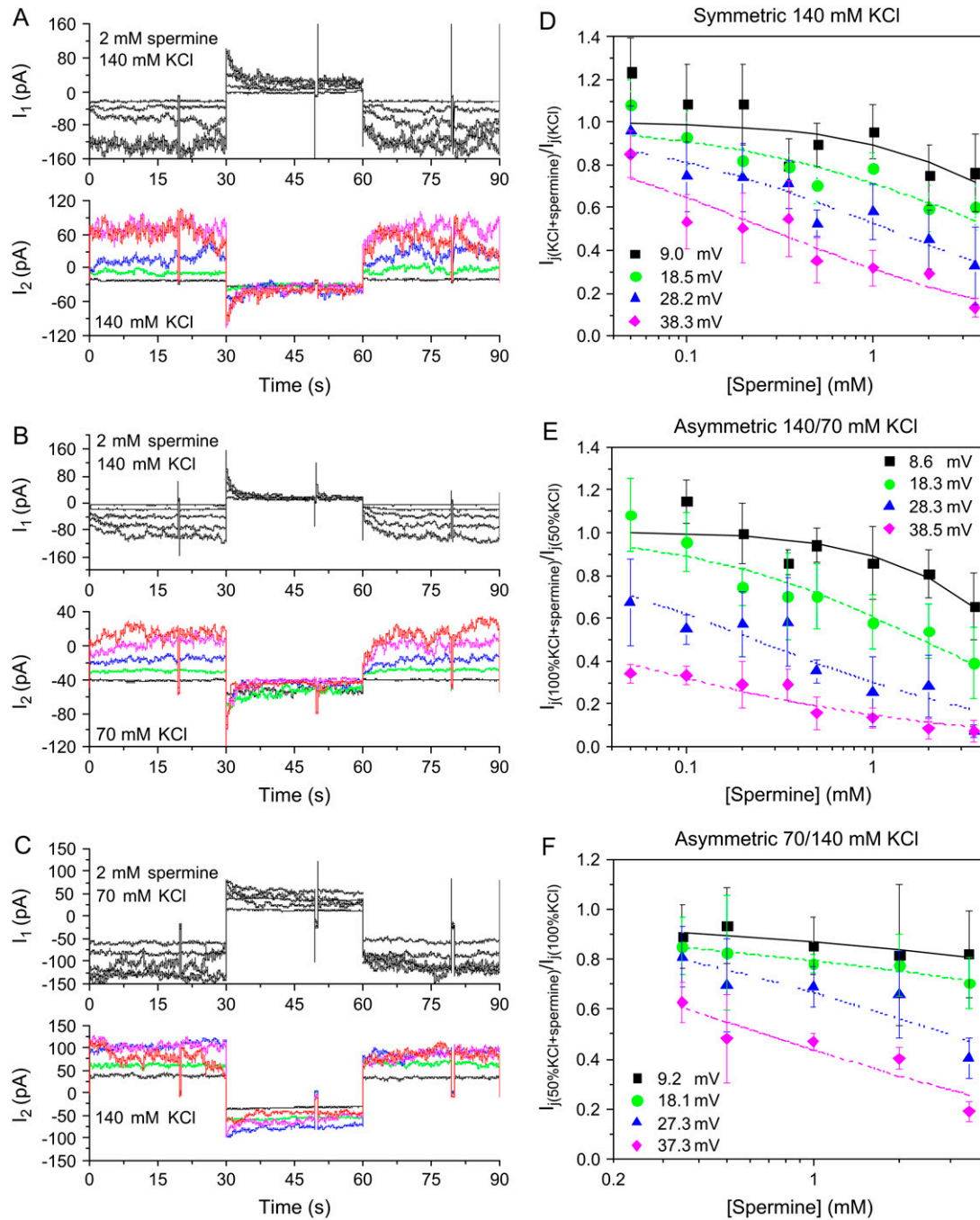$^{\ddagger}G_{max}$ was not fixed to a value of 1.0 at $V_j = 0$ mV for the indicated Boltzmann equation curve fits.

FIGURE 2 Double whole-cell current (I_1 and I_2) recordings and spermine dose-response curves under different [KCl] conditions. I_1 and I_2 recordings for the control symmetric 140 mM KCl (A), asymmetric 70/140 mM *trans/cis* KCl (B), or asymmetric 140/70 mM *trans/cis* KCl (C) conditions were obtained with 2 mM spermine added unilaterally to cell 1. Junctional current ($I_j = -\Delta I_2$ measured from baseline $V_j = 0$ mV steps) was reduced in a time-dependent manner only when a positive V_j pulse (middle 30-s pulse) was applied to cell 1. Each colored current trace represents a ± 10 mV increase in V_j (*black* < *green* < *blue* < *magenta* < *red*). The Cx40 spermine inhibition dose-response curves were calculated from the mean ($\pm$SD) fractional $I_{j(KCl + spermine)}/I_{j(KCl)}$ values for the symmetric 140 mM KCl (D), asymmetric 140/70 mM *cis/trans* KCl (E), or asymmetric 70/140 *cis/trans* mM KCl (F) conditions. The solid lines represent the Hill equation (Eq. 2) fits for each curve. The effective K_d values are listed in Table 2 (see text and Supplementary Material, Figs. S1 and S2 for more details).

of the I_j-V_j relationship between $-20 \le V_j \le -5$ mV, where the V_j-dependent gating was minimal. These procedures were followed for the 25%, 50%, or 75% reductions in [KCl] on the *cis*, *trans*, or both sides of the Cx40 gap junction. In a single experiment, a 50% reduction in [KCl] on the *trans*

side (70 mM KCl in the non-spermine-containing cell = I_2) is observed to enhance the block by spermine (Fig. 2 *B*), whereas a 50% reduction in [KCl] on the *cis* side (70 mM KCl in the spermine-containing cell 1) diminished the block (Fig. 2 *C*). The average spermine dose-response curves

TABLE 2 Symmetrical KCl V_j-dependent K_d values for spermine inhibition of Cx40 I_j

V_j (mV)	Equilibrium dissociation constant, K_d (mM)			
	100% [KCl]	75% [KCl]	50% [KCl]	25% [KCl]
9.0 ± 0.1 (r)	9.46 ± 11.5 (0.87)	59.0 ± 21.1 (0.98)	16.0 ± 3.8 (0.98)	15.5 ± 3.2 (0.98)
13.8 ± 0.1 (r)	8.9 ± 6.2 (0.91)	11.1 ± 2.7 (0.97)	5.6 ± 0.9 (0.97)	5.9 ± 1.2 (0.97)
18.6 ± 0.1 (r)	5.3 ± 2.7 (0.91)	3.7 ± 0.3 (0.98)	2.1 ± 0.2 (0.97)	1.8 ± 0.2 (0.96)
23.5 ± 0.2 (r)	2.3 ± 0.5 (0.93)	1.8 ± 0.2 (0.96)	0.94 ± 0.13 (0.94)	0.76 ± 0.07 (0.95)
28.4 ± 0.2 (r)	1.2 ± 0.2 (0.91)	0.72 ± 0.08 (0.94)	0.47 ± 0.05 (0.93)	0.40 ± 0.03 (0.95)
33.4 ± 0.2 (r)	0.59 ± 0.19 (0.82)	0.40 ± 0.05 (0.92)	0.27 ± 0.03 (0.93)	0.22 ± 0.02 (0.94)
38.4 ± 0.2 (r)	0.27 ± 0.06 (0.85)	0.28 ± 0.03 (0.93)	0.18 ± 0.02 (0.93)	0.16 ± 0.01 (0.93)
43.5 ± 0.2 (r)	0.11 ± 0.03 (0.84)	0.22 ± 0.02 (0.93)	0.15 ± 0.01 (0.92)	0.13 ± 0.01 (0.93)
48.4 ± 0.2 (r)	0.094 ± 0.047 (0.75)	0.21 ± 0.02 (0.92)	0.16 ± 0.02 (0.90)	0.13 ± 0.01 (0.91)

obtained under asymmetric 70 mM *trans* or *cis* [KCl] conditions are illustrated in Fig. 2, *E* and *F*. The V_j-dependent K_d^{eff} values for all low *cis* or *trans* [KCl] spermine dose-response curves are provided in Table 3. Unilateral *trans* [KCl] reductions decreased the V_j-dependent spermine K_d^{eff} values, whereas *cis* [KCl] reductions progressively increased the K_d^{eff} values. There were only minor changes in the spermine Hill coefficients except for the 35 mM *cis* [KCl] conditions where *n* increased to ≥1.0 (see Supplementary Material, Tables S1 and S2).

The validity of the experimentally derived spermine dose-response curves and K_d^{eff} values were assessed by modeling the normalized I_j-V_j curves for the concentration-dependent spermine block observed under each set of experimental conditions (Fig. 3). The experimental protocol is schematically diagrammed in Fig. 3 *A* such that a positive V_j on the spermine-containing side of the gap junction (*cis* = cell 1) corresponds to the right side of the I_j-V_j curve. The symbols represent the actual normalized mean I_j value for the indicated [spermine] and V_j values under the specified [KCl] conditions. The curved lines were calculated using the following Boltzmann equation for negative V_j values:

$$
\begin{aligned}
I_{j(KCl)} &= G_j \times V_j \\
&= V_j \times (G_{j,max} \times (\exp(A \times (V_j - V_{1/2}))) + G_{j,min})/ \\
&\quad (1 + (\exp(A \times (V_j - V_{1/2})))),
\end{aligned} \tag{5}
$$

and a different expression for positive V_j values in the presence of spermine:

$$
\begin{aligned}
I_{j(KCl+spermine)} &= V_j \times (G_{j,max} \times (\exp(A \times (V_j - V_{1/2}))) + G_{j,min})/ \\
&\quad (1 + (\exp(A \times (V_j - V_{1/2})))) \\
&\quad \times (1/(1 + ([spermine]/K_d^{eff})^n)),
\end{aligned} \tag{6}
$$

using the K_d^{eff} values provided in Tables 2 and 3. These I_j-V_j relationships demonstrate the shift toward lower spermine concentrations with 50% [KCl] reductions on the *trans* (non-spermine-containing) side and toward higher spermine concentrations with 50% [KCl] reductions on the *cis* (spermine-containing) side. There is reasonable agreement between the average data and the modeled fits of the I_j-V_j relationships for the various experimental conditions illustrated in Fig. 3. Overall, these observations indicate that lowering [KCl] on the *trans* or *cis* side, respectively, increased or decreased the V_j-dependent affinity of Cx40 gap junctions for spermine at positive potentials.

Mechanistic basis for spermine inhibition of Cx40 gap junctions

Macroscopic I_j recordings provide for the determination of the K_d^{eff} values and first-order kinetics, but do not provide an indication of whether the spermine inhibition results from

TABLE 3 Asymmetric KCl V_j-dependent spermine equilibrium dissociation constants (K_d^{eff})

V_j (mV)	Effective equilibrium dissociation constant, K_d^{eff} (mM)					
	25% *trans* [KCl]	50% *trans* [KCl]	75% *trans* [KCl]	75% *cis* [KCl]	50% *cis* [KCl]	25% *cis* [KCl]
4.3 ± 1.1 (r)	—	—	—	—	30.95* ± 9.22 (0.96)	4.35 ± 0.61 (0.95)
8.9 ± 1.0 (r)	4.50 ± 1.41 (0.91)	6.01 ± 5.61 (0.84)	21.3* ± 5.3 (0.95)	9.09 ± 5.16 (0.94)	20.02* ± 4.68 (0.96)	5.91 ± 0.41 (0.99)
13.6 ± 0.9 (r)	2.53 ± 0.25 (0.96)	3.61 ± 1.37 (0.89)	6.37* ± 1.91 (0.91)	10.3 ± 3.12 (0.97)	13.63* ± 2.29 (0.96)	6.77 ± 0.76 (0.98)
18.3 ± 0.8 (r)	1.68 ± 0.30 (0.92)	1.82 ± 0.44 (0.90)	2.87 ± 1.39 (0.88)	8.13 ± 2.36 (0.96)	9.01* ± 1.93 (0.94)	6.80 ± 1.89 (0.96)
23.1 ± 0.7 (r)	0.599 ± 0.163 (0.85)	0.633 ± 0.109 (0.89)	1.24 ± 0.33 (0.89)	3.86 ± 0.58 (0.96)	7.13 ± 2.78 (0.95)	4.62 ± 0.87 (0.95)
28.1 ± 0.7 (r)	0.211 ± 0.075 (0.80)	0.233 ± 0.055 (0.84)	0.603 ± 0.112 (0.90)	1.73 ± 0.43 (0.89)	2.96 ± 0.91 (0.91)	2.95 ± 0.51 (0.93)
33.1 ± 0.6 (r)	0.086 ± 0.023 (0.83)	0.049 ± 0.033 (0.73)	0.327 ± 0.049 (0.89)	0.664 ± 0.150 (0.87)	1.42 ± 0.28 (0.89)	2.22 ± 0.36 (0.91)
38.1 ± 0.5 (r)	0.076 ± 0.012 (0.87)	0.017 ± 0.008 (0.84)	0.188 ± 0.040 (0.83)	0.394 ± 0.092 (0.84)	0.674 ± 0.135 (0.88)	1.43 ± 0.34 (0.83)
43.2 ± 0.5 (r)	0.091 ± 0.020 (0.77)	0.007 ± 0.005 (0.84)	0.138 ± 0.012 (0.94)	0.149 ± 0.045 (0.85)	0.462 ± 0.087 (0.86)	1.16 ± 0.26 (0.82)
48.2 ± 0.4 (r)	0.070 ± 0.018 (0.83)	0.008 ± 0.002 (0.94)	0.163 ± 0.043 (0.81)	0.067 ± 0.039 (0.82)	0.384 ± 0.069 (0.87)	0.831 ± 0.291 (0.69)

*The Hill coefficient for the indicated dose-response curves was fixed to the mean value of 0.7.
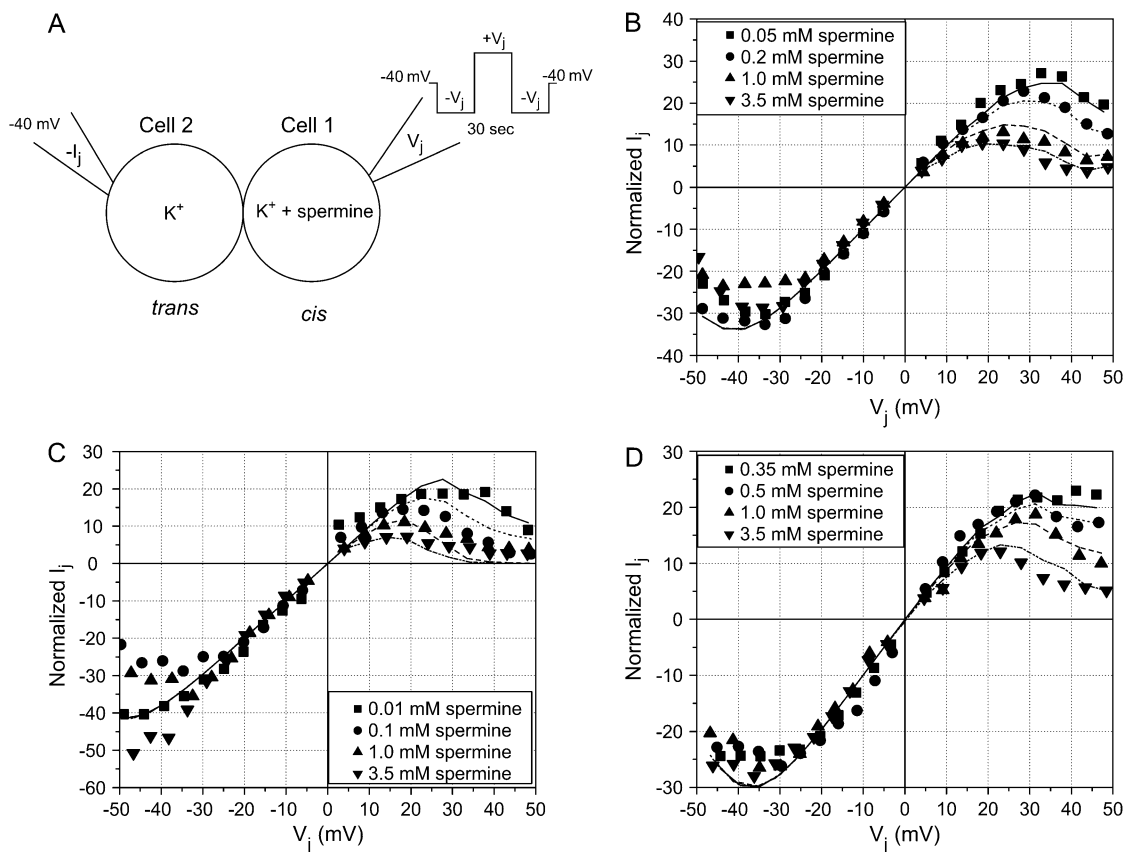
FIGURE 3 Spermine inhibition I_j-V_j relationships under three different [KCl] conditions. (*A*) Schematic diagram of the experimental design for the asymmetric [KCl] and [spermine] experiments performed on homotypic wild-type rat Cx40 gap junctions expressed in N2a cells. The normalized steady-state I_j-V_j curves for representative spermine concentrations are shown for the symmetric 140 mM KCl (*B*), asymmetric 140/70 mM *cis/trans* KCl (*C*), or asymmetric 70/140 *cis/trans* KCl (*D*) conditions. Each data point represents the average from three to five experiments (average of 4.6 ± 0.6 experiments for each [spermine] tested). The solid lines represent the model I_j-V_j curves using Eqs. 5 or 6 that account for the V_j-dependent gating plus spermine block of Cx40 gap junctions under the indicated conditions.

reductions in Cx40 channel open probability (P_{open}) or unitary gap junction channel conductance (γ_j). To determine which of these mechanisms was most responsible for the reduction in Cx40 I_j under the altered transjunctional [KCl] conditions, low g_j recordings from four experiments with high-dose (3.5 mM) or low-dose (100 μM) spermine and opposite *cis-trans* [KCl] conditions were analyzed to determine the effects on Cx40 gap junction channel activity and γ_j (Fig. 4). The high-dose spermine maximizes any possible effect of spermine on γ_j. The cumulative open probabilities ($N \times P_{open}$) of the summatory channel activities during the 30-s negative V_j (nonblocking) and subsequent positive V_j (blocking) steps were calculated to provide a direct measure of the relative channel P_{open} under the distinctly different experimental conditions. The time integral of the total I_j was divided by the V_j pulse duration integral of the unitary current ($i_j = g_j \times V_j$) to arrive at the $N \times P_{open}$ calculation. In the absence of spermine, P_{open} was found to be identical for the 148-pS Cx40 gap junction channels observed during the $-V_j$ and $+V_j$ pulses under control [KCl] conditions (Fig. 4 *A*). A 25% reduction in the *trans* [KCl] produced a 15% decrease

in P_{open} at $+V_j$ relative to the $-V_j$ pulse, whereas the apparent γ_j values were reduced from 148 to 109 pS on the *trans* side of the junction (Fig. 4 *B*). The "apparent" γ_j values were calculated by dividing i_j for each observable channel by the command V_j value (i.e., $V_1 - V_2$). The actual γ_j values would require accounting for the reversal potential shift due to the asymmetric [KCl] gradients that averaged -6.2, -14.4, and -26.5 mV for the 75%, 50%, and 25% *trans* [KCl] conditions, respectively, as determined previously for the Cx40 gap junction channel (19). The complete i_j-V_j relationships for the experimental conditions illustrated in Fig. 4 are provided as Supplemental Material (Fig. S6).

In the presence of 3.5 mM spermine, $N \cdot P_{open}$ was reduced by 70% during the $+35$ mV V_j pulse in the control (symmetrical 140 mM [KCl]) experiment (Fig. 4 *C*). The apparent γ_j values were reduced by 14% (128/148 pS) under these conditions, in close agreement with our previous observations in the presence of 2 mM spermine (6). Lowering the *trans* [KCl] to 105 mM reduced the apparent γ_j to $\sim$114 pS during the negative V_j pulse (Fig. 4 *D*). However, the $N \cdot P_{open}$ value during the $+35$ mV V_j pulse in the 75% *trans* KCl
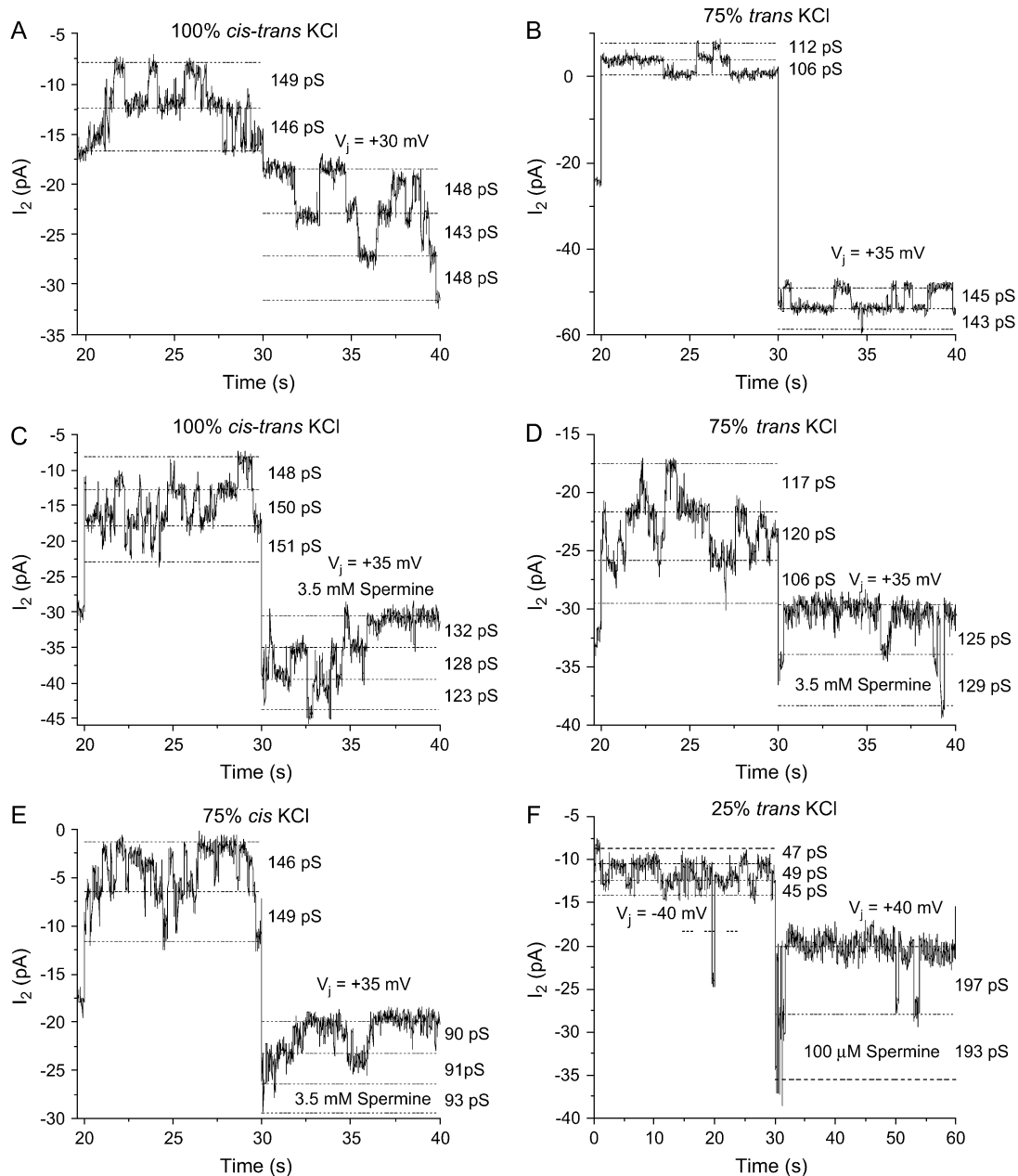
FIGURE 4 Channel activity in the presence or absence of spermine and unilaterally reduced transjunctional [KCl] gradients. (A) Cx40 channel activity under symmetrical 140 mM [KCl] conditions in the absence of spermine. The activity of zero to three 148 pS channels is evident and the cumulative open probabilites ($N \times P_{open}$) were identical for each 30-s $\pm$30-mV pulse with an average of 1.02 channels being open for the entire duration of each pulse. (B) The cumulative open probability at +35 mV (6.5 open channels) was reduced by 14% relative to the −35-mV V_j pulse (5.6 open channels) under 75% *trans* [KCl] conditions in the absence of spermine. The apparent single-channel conductance (γ_j) was still 144 pS for the *cis*-side positive and was reduced to 109 pS for the *trans*-side positive. (C–F). Cx40 channel activity observed during the last 10 s of a 30-s-duration V_j pulse to −35 mV and the first 10 s of the following +35-mV V_j pulse in the presence of 3.5 mM spermine. (C) The γ_j of the observed channel activity with symmetrical 140 mM [KCl] measured 128 pS in the presence of spermine. This corresponds to a 15% reduction in γ_j, whereas $N \times P_{open}$ was reduced by 70% during the positive V_j pulse (0.96 relative to 3.14 open channels; $+V_j/-V_j$) in the presence of 3.5 mM spermine. (D) In this example, the *trans* side of the gap junction contained only 105 mM KCl. This reduced the apparent *trans* γ_j slightly (?20%) to 120 pS but $N \times P_{open}$ declined by 81% (0.42 relative to 2.21 open channels) during the +35-mV V_j step on the *cis* spermine-containing side of the junction. (E) Results obtained when [KCl] was reduced to 105 mM on the *cis* 3.5 mM spermine-containing side of the gap junction. $N \times P_{open}$ declined by only 45% (1.13 relative to 2.47 open channels) during the +35-mV step, whereas the apparent γ_j was reduced by 25% to 90 pS. (F) Cx40 gap junction channel blockade at low (100 μM) [spermine] occurred by a 96% reduction in $N \times P_{open}$ relative to the preceeding −40 mV V_j step (0.24 relative to 3.89 open channels). This dramatic reduction in $N \times P_{open}$ occurred despite the apparently higher γ_j value of 195 pS on the *cis* spermine-containing side of the junction due to the electrodiffusion potential established by the asymmetric [KCl] gradient. The dotted line indicates the true zero I_j baseline under these recording conditions (see text for further details).

experiment was diminished by 81%, more than under control conditions. Similar analysis of the *cis* 105 mM [KCl] plus 3.5 mM spermine experiment indicated a further reduction in the apparent γ_j to 91 pS (a 29% reduction from 128 pS), but the $N \times P_{open}$ value was reduced by only 55% (Fig. 4 *E*). These multi-channel recording were obtained at spermine concentrations several times higher than the V_j-dependent K_d^{eff} under these experimental conditions (Table 2). To ascertain whether the same mechanism of block applies at low spermine concentrations, Cx40 gap junction channel recordings were examined at spermine doses that closely approximated the experimental K_d^{eff} value. Fig. 4 *F* demonstrates a 94% reduction in the $N \cdot P_{open}$ value in the presence of 100 μM spermine under 25% *trans* [KCl] conditions, despite the increased apparent γ_j. Under symmetrical 25% KCl conditions, the Cx40 gap junction channel γ_j was 70 pS and the average slope γ_j of the 25%/100% i_j-V_j relationship was 108 pS, close to the arithmetic mean of 70 and 148 pS (data not shown) (19). These results consistently demonstrate that the predominant basis for the reductions in macroscopic I_j during the spermine experiments with altered transjunctional KCl and spermine concentrations was the decrease in the cumulative gap junction channel activity, $N \cdot P_{open}$.

Effects of [KCl] on the spermine blocking kinetics

Since the K_d^{eff} values decreased concomitantly with the decreases in [KCl] on the opposite side of the junction relative to spermine, the relative association rates (K_{on}) and dissociation rates (K_{off}) should be altered up or down by the reduction in the *cis* or *trans* [KCl] in accordance with the definition: $K_d^{eff} = K_{off}/K_{on}$. The spermine K_{on} values were calculated using the expression

$$K_{on} = (1 - P_{open})/(\tau_{decay} \times [\text{spermine}]), \qquad (7)$$

which accounts for the varying [spermine] and amount of inhibition observed at each V_j. P_{open} was the fraction of I_j that remained at the end of the positive V_j pulse, and the decay time constant ($\tau_{decay} = 1/(K_{on} + K_{off})$) was determined by fitting the decay phase of I_j during the positive V_j steps with a first-order exponential function (Fig. 5 *A*). The corresponding off-rates (K_{off}) were calculated from the expressions

$$K_{off} = P_{open}/\tau_{decay}, \qquad (8)$$

at positive V_j and

$$K_{off} = 1/\tau_{rise} \qquad (9)$$

at negative V_j (where $P_{open} = 1$). τ_{rise} was determined by fitting the rising phase of I_j and (Fig. 5 *B*). The calculated on-rates (in ms$^{-1} \cdot$ mM^{-1}) and off-rates (in ms^{-1}) under symmetrical [KCl] conditions were plotted as a function of V_j, and the pooled data were fit with a single exponential function of the form

$$K = A \times \exp((V_j - V_{init})/V_k) + C, \qquad (10)$$

where A is the initial amplitude, V_{init} is the minimum V_j value from which kinetic measurements could be determined, V_k defines the V_j-dependence of the spermine on- or off-rates, and C is a constant (Fig. 5, *C* and *D*). The spermine on-rate and off-rate results obtained under asymmetric [KCl] conditions are similarly illustrated in Fig. 6 (see Supplementary Material, Fig. S4). It is apparent that the spermine K_{on} rates increased and the K_{off} rates decreased as [KCl] was lowered symmetrically or on the opposite *trans* side of the gap junction. When *cis* [KCl] was lower relative to the normal-[KCl] opposite side of the junction, the spermine K_{on} rates were diminished. The spermine K_{off} rates varied reciprocally in all cases. These data are consistent with transjunctional K$^+$ flux opposing the association of spermine with the Cx40 gap junction channel.

K$^+$ activity dependence of Cx40 spermine inhibition

The observations presented thus far suggest that spermine associates with the Cx40 gap junction channel while experiencing positive V_j gradients, and that transjunctional K$^+$ flux opposes this interaction. To examine this hypothesis further, we employed the Woodhull model to calculate the ''effective electrical distance'' of a charged molecule to the site of occlusion (30,31). According to the model, voltage-dependent inhibitory K_d values result from point charges on a blocking molecule sensing a fraction of the applied voltage field at the site of occlusion. For a gap junction channel, the actual applied V_j field results from the difference in cellular membrane potentials ($V_j = [(V_1 + \Delta V_1) - (I_1 \times R_{el1}) - V_2 + (I_1 \times R_{el1})]$) (Eq. 1). In the case of asymmetric [KCl] gradients, K$^+$ ions will experience an electrodiffusion potential that will affect spermine binding if there is a common site of interaction. The electrical distance (δ) is defined by the equation

$$K_d^{eff} = (b_{-1}/b_1)\exp(-z\delta FV_j/RT) + C. \qquad (11)$$

The spermine dissociation/association rate ratio (b_{-1}/b_1) is equal to the effective spermine K_d in the absence of an applied V_j ($K_d^{eff}(0)$), z is the effective valence, δ is the fraction of the applied V_j field at the inhibitory site, and C is a constant remainder term. The product of $z\delta$ ranged from 2.4 to 5.6 depending on whether the 25% KCl was on the side with or without the added spermine (see Supplemental Material, Fig. S5). Spermine has a valence of +4 at physiological pH, so the equivalent δ for all four point charges was 1.06 ± 0.09 under the control symmetric 140 mM KCl conditions. The δ-value increased slightly to 1.21 ± 0.12 with symmetrical lowering of [KCl] to 35 mM. The δ-value increased even further to 1.4 when [KCl] was lowered unilaterally, even though the *cis* spermine-containing side of the junction contained 140 mM [KCl]. Conversely, the δ-value decreased to 0.6 when [KCl] was unilaterally reduced to 35 mM on the *cis* side of the gap junction.
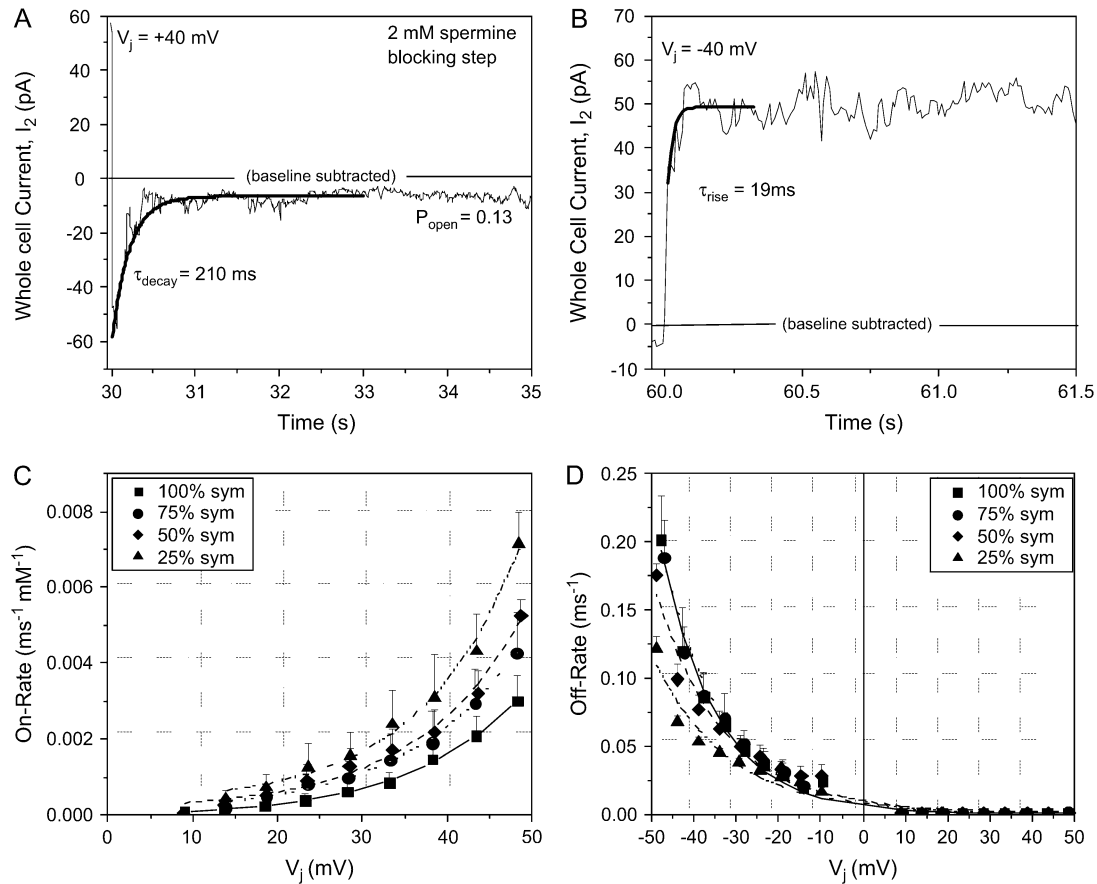
FIGURE 5 Concentration- and V_j-dependent spermine association and dissociation rates under symmetric [KCl] conditions. (*A*) Determination of the decay time constant (τ_{decay}) during the onset of a positive V_j step in the presence of 2 mM spermine. For this example, the steady-state open probability (P_{open}) was 0.11. (*B*) Determination of the rise-time constant (τ_{rise}) during the onset of a negative V_j step in the presence of 2 mM spermine. (*C*) The spermine on-rates (K_{on}), determined from the I_j decay time constants at $+V_j$ values, were calculated using Eq. 7 for all four symmetric [KCl] conditions. The K_{on} values were fit by a single exponential. (*D*) The spermine off-rates (K_{off}), calculated from the decay time constants at $+V_j$ values or rising time constants at $-V_j$ values using Eq. 8 or 9, respectively, were fit by a single exponential function for all four symmetric [KCl] conditions. Symmetrically decreasing the [KCl] reciprocally increased and decreased the spermine on-rates and off-rates (see Supplemental Material, Fig. S3, for further details).

To examine any possible correlation between the δ-value and the *cis/trans* K$^+$ activity ratio, the corresponding curve was fitted with the Hill equation

$$v^\delta = v^\delta_{max}/(1 + (K^+_{1/2}/[cis/trans])^n). \qquad (12)$$

In Fig. 7, the Hill coefficient (*n*) was 0.99 ± 0.16 with a v^δ_{max} of 1.64 ± 0.13 and a half-maximal *cis/trans* K$^+$ activity ratio ($x_{1/2}$) of 0.53 ± 0.09, assuming a net valence of $+4$ ($r = 0.97$). This correlation is indicative of a direct relationship between the *cis/trans* K$^+$ activity ratio and the fraction of the V_j field sensed at the inhibitory site for spermine. Also plotted are the δ-values for the symmetrical 75%, 50%, and 25% reductions in [KCl] (*open squares*) for comparative purposes. Decreasing the *cis* [KCl] to match the reduced *trans* [KCl] would enhance any electrostatic effect of the channel protein surface charge on spermine association by decreasing the ionic strength of the cytoplasmic solution. These symmetrical low [KCl] data do indicate an increased δ-value com-

pared to the control 140 mM KCl condition, but the dashed arrows indicate the reduction in the δ-value at the same ionic strength when the *trans* reduction in [KCl] is matched on the *cis* side of the gap junction. The on- or off-rate voltage constants (V_k) under different experimental conditions were also plotted relative to the *cis/trans* K$^+$ activity ratios and fitted with the Hill equation

$$v^{V_k} = v^{V_k}_{max}/(1 + (K^+_{1/2}/[cis/trans])^n) + C. \qquad (13)$$

The respective Hill coefficients were 3.4 ± 0.5 and 3.5 ± 0.1, the half-maximal *cis/trans* K$^+$ activity ratios ($x_{1/2}$) were 0.99 ± 0.01 and 1.22 ± 0.06, and the values of C were -17.7 ± 0.1 and 9.8 ± 0.3 mV for the off-rate and on-rate V_k values, respectively. These Hill coefficient values are similar to the valence of spermine ($z = +4$ at pH 7.4) and are consistent with the hypothesis that the equivalent of one spermine molecule is sufficient to produce the block of Cx40 gap junctions. The larger increase in the δ-value under low
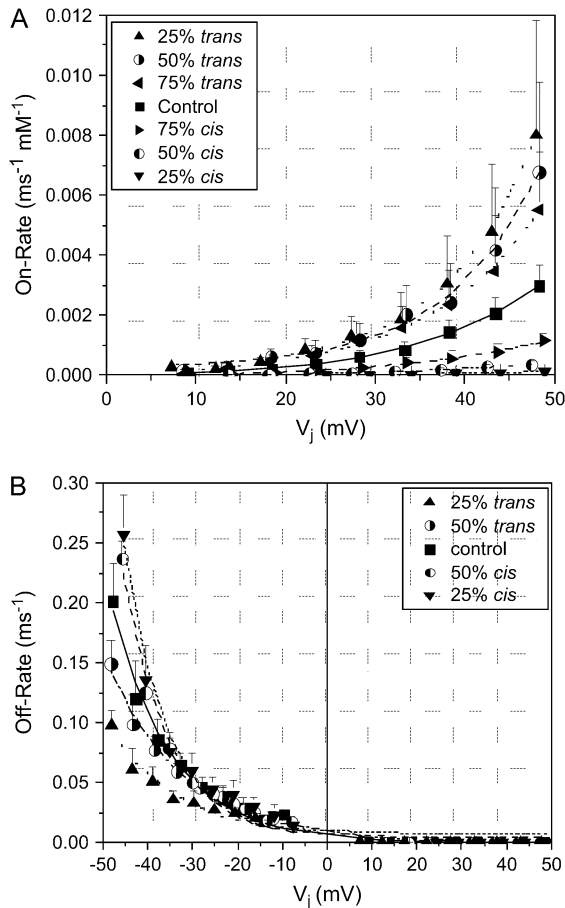
A

B

FIGURE 6   Concentration- and V_j-dependent spermine association and dissociation rates under asymmetric [KCl] conditions. (*A*) The spermine K_{on} rates, determined from τ_{decay} and P_{open} at $+V_j$ values for all asymmetric *cis/trans* [KCl] conditions, were well described by a single exponential function (Eq. 10). Increasing the *cis/trans* [KCl] ratio increased the spermine on-rates, whereas decreasing it had the opposite effect. (*B*) The spermine K_{off} rates, calculated from τ_{decay} and P_{open} at $+V_j$ or τ_{rise} values at $-V_j$ values for all asymmetric *cis/trans* [KCl] conditions, were well described by Eq. 10. Increasing the *cis/trans* [KCl] ratio reciprocally increased the spermine on-rates and decreased the spermine off-rates and vice versa (see Supplementary Material, Fig. S4 for further details).

trans [KCl] conditions relative to the symmetrical situation indicates that net transjunctional K^+ flux is more influential than the enhanced electrostatic effects of decreasing the monovalent ionic strength of the internal milieu on the spermine inhibitory block.

DISCUSSION

The purpose of this study was to explore further the ionic basis for the inhibition of Cx40 gap junction currents by intracellular spermine. Previous results have shown that this property is specific to Cx40 compared to Cx43 and results predominantly from decreased Cx40 gap junction channel open probability with increasing [spermine] and positive trans-junctional voltages (6). Spermine inhibition also involves
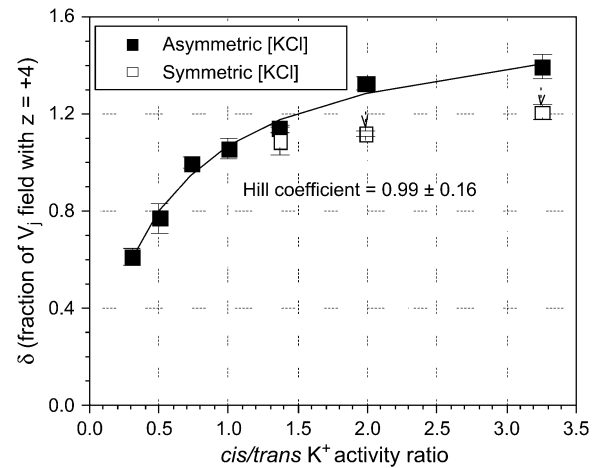

FIGURE 7 δ-Values (■) for control and all asymmetric experimental *cis/trans* [KCl] conditions. The fraction of the V_j field (δ) sensed by spermine ($z = +4$) at the inhibitory site increased with elevations in the *cis/trans* K^+ activity ratio with a Hill coefficient of 0.99 ± 0.16, indicative of a direct single-site interaction (see Supplementary Material, Fig. S5 for further details). The δ-value under symmetrically reduced [KCl] conditions (□) was less than that observed during the *trans*-only reduction. The shift in the δ-value from the low *trans* condition to the equivalent low *cis-trans* condition is indicated by the dashed arrow.

Cx40 amino terminal (NT) acidic and basic amino acid residues that are distinct between Cx40 and Cx43 (18,19). Two general mechanisms are considered for ionic block of ion channels, direct pore block characterized by reductions in unitary channel conductance (γ_j) and discrete blocking events characterized by prolonged closed intervals and reduced open probabilities (P_{open}) during channel gating at a constant voltage. The latter is sometimes referred to as a ''gating'' type of block. The gating mechanism of block was previously indicated for the Cx40 gap junction channel since 2 mM spermine added unilaterally to one side of the gap junction reduced P_{open} by 95% yet reduced γ_j by only 15% (6). The major question to be considered here is whether this spermine inhibition of Cx40 I_j results from a direct action on the channels or from an allosteric alteration of the intrinsic V_j-dependent gating of the gap junctions. To accomplish this, we altered the [KCl] both bilaterally and unilaterally in the presence of spermine applied unilaterally to homotypic Cx40 gap junctions and determined the effective K_ds and on- and off-rate kinetics for spermine block. In this article, we report the effects of ionic strength alterations and transjunctional [KCl] gradients on the equilibrium binding properties and kinetics for spermine inhibition of Cx40 gap junctions.

Symmetrical reductions in [KCl] decreased the K_d for spermine inhibition of Cx40 I_j. These values were determined by fitting the V_j-dependent spermine dose-response curves with the Hill equation for cooperative binding (Eq. 3, Fig. 2). Only small decreases in the spermine K_d values were produced by bilateral low [KCl]. These results indicate that electrostatic attraction is not the major determinant of spermine

affinity since the Debye length constant would be expected to increase with decreasing ionic strength, thus reducing the spermine K_d values. The Hill coefficients for spermine inhibition were <1 and did not change significantly with these bilateral reductions in [KCl]. The lack of change in the Hill coefficients further suggests that K^+ ions are not the basis for the negative cooperativity of spermine inhibition (Hill coefficient, $n \cong 0.6$, see Supplemental Material, Figs. S1 and S2). The Hill coefficient for spermine inhibition achieved independence ($n = 1.0$) only when *cis* [KCl] was threefold lower than *trans* [KCl], a condition that elevated the spermine K_d values. These results are consistent with negative cooperativity among inhibitory spermine molecules that is alleviated by higher net transjunctional K^+ fluxes. Negative cooperativity among spermine molecules independent of ionic strength was observed with the BK channel (20). This led to the hypothesis that multiple-site interactions among spermine molecules were responsible for this negative cooperativity. It is feasible to assume that the Cx40 gap junction channel also contains multiple spermine inhibitory sites since each of the six Cx40 NT domains contains four acidic residues within a span of eleven amino acids. It is not precisely known if more than one Cx40 NT domain or if other cytoplasmic domains are required for block to occur, but the hexameric configuration of connexin subunits raises the possibility that multiple spermine blocking sites can exist within the same Cx40 gap junction channel.

The kinetics of spermine block were also altered by the symmetrical decreases in [KCl], which is expected from the changes in the observed K_ds. The spermine on-rates increased progressively and the off-rates decreased progressively as [KCl] was symmetrically reduced (Fig. 5). The k_{on} values became more V_j-sensitive and the k_{off} values less sensitive as bilateral [KCl] was decreased. These alterations are consistent with transjunctional K^+ flux opposing spermine block. One mechanism by which the V_j-dependent kinetic shifts could occur is if K^+ ions and spermine^{4+} molecules compete for common sites on the Cx40 channel. These ion conductive and spermine inhibitory sites must reside somewhere on the Cx40 protein that affects V_j-dependent gating more than channel conductance since the predominant effect of transjunctional spermine and KCl gradients was on Cx40 gap junction channel open probability rather than γ_j (Figs. 1 and 4). This conclusion is substantiated by the observation that the 10–15% reduction in G_j at +40 mV with 75% *trans* [KCl] in Fig. 1 closely matches the observed decrease in Cx40 channel $N{\cdot}P_{open}$ under identical conditions in Fig. 4 *B*. The highest concentrations of spermine reduced γ_j by only 15–30%, depending on the *cis* [KCl], whereas $N{\cdot}P_{open}$ was observed to decrease by 45–94%, depending on the *cis-trans* [KCl] gradient (Fig. 4, *C–E*) (6).

Asymmetric alteration of the internal [KCl], performed while maintaining osmotic balance (ignoring the added spermine to one side of the gap junction) imposes a KCl electrodiffusion potential across the gap junction in addition to the alterations in ionic strength. These lowered *trans* or *cis* (relative to the spermine-containing and V_j-pulsed side (see Fig. 3)) [KCl] experiments produced much lower or higher spermine K_d values than under symmetrical conditions. The effective K_ds were calculated from the V_j-dependent I_j(KCl + spermine)/I_j(KCl) curves after accounting for the alterations in the V_j-dependent gating produced by the asymmetric [KCl] (Fig. 1 and Table 1). These K_d^{eff} determinations are central to the question of whether spermine directly inhibits, or whether it ''enhances'', the V_j-dependent gating of the Cx40 gap junction channel. By accounting for the V_j-dependent gating properties of the homotypic Cx40 gap junctions while experiencing asymmetric [KCl] gradients, any further V_j-dependent asymmetries in the I_j-V_j relationships must be the result of spermine inhibition occurring at positive V_j values (Fig. 3). The spermine on- and off-rate kinetics were oppositely affected by the *cis/trans* [KCl] gradients. Again, decreasing *trans* [KCl] increased the spermine association (k_{on}) rates and V_j-dependence while decreasing the spermine dissociation (k_{off}) rates and V_j-dependence (Fig. 6). The opposite effects were observed with decreases in the *cis* [KCl], as expected. That the V_j-sensitivity and spermine on-off rate kinetics were affected more by unilateral than bilateral *cis* or *trans* [KCl] reductions is again consistent with net increases or reductions in transjunctional K^+ flux diminishing or enhancing spermine association from the *cis* side of the gap junction. These results cannot definitively determine whether spermine itself is acting as the inactivation gating particle or whether spermine is modulating the behavior of an intrinsic V_j gating particle. Additional experiments with polyamine analogs and site-directed functional mutagenesis studies of connexin sequences will be required to further delineate between these two hypotheses.

The hypothesized K^+-dependence of Cx40 spermine inhibition was further examined by measuring the actual K^+ activities of the 25%, 50%, and 75% of normal [KCl] internal pipette solutions and determining the relationship between the fraction of the applied V_j field (δ) or the kinetic on- and off-rate voltage constants ($V_{k,\,on\,or\,off}$) and the *cis/trans* K^+ activity ratio (Fig. 7 and Supplemental Material, Fig. S5). After accounting for an equivalent valence of +4, the fractional electrical distance δ estimate varied according to the *cis/trans* K^+ activity ratio, with a Hill coefficient of 0.99. These estimated parameters also assumed an extrapolated minimum $\delta = 0$ in the absence of *cis* K^+ and a maximum $\delta = 1.6$ in the absence of *trans* K^+. We do not know if these theoretical limitations of the equivalent electrical distance analysis are true experimentally, but it is feasible to assume that a large *trans* K^+ flux can completely oppose the inhibition by *cis* spermine. A $z\delta$-value >4 implies that more than one spermine molecule can enter the Cx40 channel at the same time when the *trans* K^+ flux is maximally reduced by a large applied V_j gradient, a high *cis* [KCl] gradient, or both. Another limitation of this δ analysis approach is that it does not provide an indication of where the charge occurs within

the channel pore or upon the inhibitory molecules. Again, this information can only be provided by subsequent structure-function analysis of mutant channel proteins in conjunction with polyamine analogs.

The observation of a spermine inhibitory Hill coefficient of 1 for the K^+-dependence of the δ estimate is consistent with a single spermine molecule accounting for all of the inhibition of Cx40 I_j at the site of occlusion. However, it cannot be ruled out that four spermine molecules each contribute one identical positive charge to the observed inhibitory response. We believe the latter hypothesis is unlikely given the knowledge that spermidine, which lacks one terminal propylamine relative to spermine, produced only partial block of Cx40 gap junctions despite significantly higher concentrations (6). The 10-fold higher K_d values, the reduced efficacy of block, and the estimated δ-value of 0.75 for spermidine all suggest that the four positively charged amino groups of one spermine molecule are necessary to effect block of Cx40 gap junctions. Still, if a single spermine molecule is sufficient to occlude a Cx40 gap junction channel, then long closed intervals and reduced channel P_{open} values should be evident at submaximal spermine concentrations. This was indeed the case, as can be seen in Fig. 4 F with 100 μM spermine. Since the Hill coefficient for spermine inhibition is 0.70 under these conditions, the negative cooperativity and low inhibitor concentration also favor blockade by a single molecule rather than multiple spermine molecules.

The K^+-dependence of the spermine electrical distance (δ) and kinetic rate constants support the hypothesis that K^+ ions and spermine^{4+} molecules directly compete for common sites on the Cx40 gap junction channel. Direct competitive inhibition is characterized by outward shifts in the K_d values with the addition of an antagonist (i.e., transjunctional K^+ flux), without reductions in the maximum effect of the drug (i.e., spermine inhibition). This is best demonstrated by the progressively lower *trans* [KCl] that continued to shift the spermine K_d values toward smaller values while achieving maximum blockade. The increase in the δ-value does not imply indirect (noncompetitive) competition between K^+ and spermine, since the data in Fig. 7 are consistent with a saturable site with no reduction in the maximum inhibitory effect of spermine in response to varying transjunctional [KCl] gradients.

In summary, the block of Cx40 gap junctions by intracellular spermine is consistent with a gating type of block that occurs within the V_j field and ion conduction pathway of the channel. The spermine inhibition is opposed by transjunctional K^+ flux and may require only single-site occupancy to occlude the channel, although multiple sites may exist. These conclusions are consistent with a particle-receptor bimolecular gating mechanism, with spermine acting as the inactivation particle or enhancing the action of an intrinsic gating particle. To date, the only Cx40 amino acid residues implicated in the spermine inhibitory process reside on the cytoplasmic amino terminus and are unique to Cx40 relative

to Cx43. The connexin amino terminal domain has previously been implicated in the V_j-dependent gating process and influences the V_j polarity of gating by virtue of sensing the applied V_j field (31–34). These new data suggest that bimolecular interactions with the connexin amino terminal domain can serve as a V_j-dependent gating mechanism with spermine acting as an exogenous (to the connexin protein) gating particle or modifier and the connexin NT domain serving as the receptor.

SUPPLEMENTARY MATERIAL

To view all of the supplemental files associated with this article, visit www.biophysj.org.

REFERENCES

1. Harris, A. L. 2001. Emerging issues of connexin channels: Biophysics fills the gap. *Q. Rev. Biophys.* 34:325–472.

2. Lampe, P. D., and A. F. Lau. 2004. The effects of connexin phosphorylation on gap junction communication. *Int. J. Biochem. Cell Biol.* 36:1171–1186.

3. Ramanan, S. V., P. R. Brink, K. Varadaraj, E. Peterson, K. Schirrmacher, and K. Banach. 1999. A three-state model for connexin37 gating kinetics. *Biophys. J.* 76:2520–2529.

4. Banach, K., S. V. Ramanan, and P. R. Brink. 2000. The influence of surface charges on the conductance of the human connexin37 gap junction channel. *Biophys. J.* 78:752–760.

5. Ebihara, L., X. Liu, and J. D. Pal. 2003. Effect of external magnesium and calcium on human connexin46 hemichannels. *Biophys. J.* 84:277–286.

6. Musa, H., and R. D. Veenstra. 2003. Voltage-dependent blockade of connexin40 gap junctions by spermine. *Biophys. J.* 84:205–219.

7. Puljung, M. C., V. M. Berthoud, E. C. Beyer, and D. A. Hanck. 2004. Polyvalent cations constitute the voltage gating particle in human connexin37 hemichannels. *J. Gen. Physiol.* 124:587–603.

8. Heby, O. 1981. Role of polyamines in the control of cell proliferation and differentiation. *Differentiation.* 19:1–20.

9. Thomas, T., and T. J. Thomas. 2001. Polyamines in cell growth and cell death: molecular mechanisms and therapeutic applications. *Cell. Mol. Life Sci.* 58:244–258.

10. Wallace, H. M., A. V. Fraser, and A. Hughes. 2003. A perspective of polyamine metabolism. *Biochem. J.* 376:1–14.

11. Ransom, R. W., and N. L. Stec. 1988. Cooperative modulation of [^{3}H]MK-801 binding to the *N*-methyl-D-aspartate receptor-ion channel complex by L-glutamate, glycine, and polyamines. *J. Neurochem.* 51:830–836.

12. Lopatin, A. N., E. N. Makhina, and C. G. Nichols. 1994. Potassium channel block by cytoplasmic polyamines as the mechanism of intrinsic rectification. *Nature.* 372:366–369.

13. Donevan, S. D., and M. A. Rogawski. 1995. Intracellular polyamines mediate inward rectification of Ca^{2+}-permeable α-amino-3-hydroxy-5-methyl-4-isoxazolepropionic acid receptors. *Proc. Natl. Acad. Sci. USA.* 92:9298–9302.

14. Uehara, A., M. Fill, P. Velez, M. Yasukochi, and I. Imanaga. 1996. Rectification of rabbit cardiac ryanodine receptor current by endogenous polyamines. *Biophys. J.* 71:769–777.

15. Lynch, J. W. 1999. Rectification of the olfactory cyclic nucleotide-gated channel by intracellular polyamines. *J. Membr. Biol.* 170:213–227.

16. Guo, D., and Z. Lu. 2000a. Mechanism of IRK1 channel block by intracellular polyamines. *J. Gen. Physiol.* 115:799–813.

17. Huang, C. J., and E. Moczydlowski. 2001. Cytoplasmic polyamines as permeant blockers and modulators of the voltage-gated sodium channel. *Biophys. J.* 80:1262–1279.

18. Musa, H., E. Fenn, M. Crye, J. Gemel, E. C. Beyer, and R. D. Veenstra. 2004. Alternate amino terminal glutamate or lysine residues of rat connexin-40 and -43 affect spermine block and voltage gating. *J. Physiol.* 557:863–878.

19. Lin, X., E. Fenn, and R. D. Veenstra. 2006. An amino-terminal lysine residue of rat connexin40 that is required for spermine block. *J. Physiol.* 570:251–269.

20. Zhang, Y., X. Niu, T. I. Brelidze, and K. M. Magelby. 2006. Ring of negative charge in BK channels facilitates block by intracellullar Mg^{2+} and polyamines through electrostatics. *J. Gen. Physiol.* 128:185–202.

21. Ficker, E., M. Taglialatela, B. A. Wible, C. M. Henley, and A. M. Brown. 1994. Spermine and spermidine as gating molecules for inward rectifier K^+ channels. *Science.* 266:1068–1072.

22. Bowie, D., and M. L. Mayer. 1995. Inward rectification of both AMPA and kainate subtype glutamate receptors generated by polyamine-mediated ion channel block. *Neuron.* 15:453–462.

23. Chao, J., N. Seiler, J. Renault, K. Kashiwagi, T. Masuko, K. Igarashi, and K. Williams. 1997. N^1-dansyl-spermine and N^1-(*n*-octanesulfonyl)-spermine, novel glutamate receptor antagonists: block and permeation of *N*-methyl-D-aspartate receptors. *Mol. Pharmacol.* 51:861–871.

24. Guo, D., and Z. Lu. 2000b. Mechanism of cGMP-gated channel block by intracellular polyamines. *J. Gen. Physiol.* 115:783–798.

25. Williams, K. 1997. Modulation and block of ion channels: a new biology of polyamines. *Cell. Signal.* 9:1–13.

26. Veenstra, R. D. 2001. Voltage clamp limitations of dual whole-cell gap junction current and voltage recordings. I. Conductance measurements. *Biophys. J.* 80:2231–2247.

27. Barrio, L. C., T. Suchyna, T. Bargiello, L. Xu, R. S. Roginski, M. V. L. Bennett, and B. J. Nicholson. 1991. Gap junctions formed by connexins 26 and 32 alone and in combination are differently affected by applied voltage. *Proc. Natl. Acad. Sci. USA.* 88:8410–8414.

28. Bruzzone, R., J. A. Haefliger, R. L. Gimlich, and D. L. Paul. 1993. Connexin40, a component of gap junctions in vascular endothelium, is restricted in its ability to interact with other connexins. *Mol. Biol. Cell.* 4:7–20.

29. Valiunas, V., R. Weingart, and P. R. Brink. 2000. Formation of heterotypic gap junctions by connexins 40 and 43. *Circ. Res.* 86:e42–e49.

30. Woodhull, A. M. 1973. Ionic blockage of sodium channels in nerve. *J. Gen. Physiol.* 61:687–708.

31. Musa, H., J. D. Gough, W. J. Lees, and R. D. Veenstra. 2001. Ionic blockade of the rat connexin40 gap junction channel by large tetraalkylammonium ions. *Biophys. J.* 81:3253–3274.

32. Verselis, V. K., C. S. Ginter, and T. A. Bargiello. 1994. Opposite voltage gating polarities of two closely related connexins. *Nature.* 368:348–351.

33. Purnick, P. E., D. C. Benjamin, V. K. Verselis, T. A. Bargiello, and T. L. Dowd. 2000a. Structure of the amino terminus of a gap junction protein. *Arch. Biochem. Biophys.* 381:181–190.

34. Purnick, P. E., S. Oh, C. K. Abrams, V. K. Verselis, and T. A. Bargiello. 2000b. Reversal of the gating polarity of gap junctions by negative charge substitutions in the N-terminus of connexin 32. *Biophys. J.* 79:2403–2415.